

<https://doi.org/10.1038/s43247-025-02013-w>

# Gross primary productivity is more sensitive to accelerated flash droughts

Check for updates

Yangyang Jing<sup>1</sup>, Shuo Wang<sup>1,2</sup>✉, Pak Wai Chan<sup>3</sup> & Zong-Liang Yang<sup>1,4</sup>

Flash droughts, characterized by their rapid onset, substantially affect terrestrial ecosystems. However, the sensitivity of ecosystem productivity to the rapid development of flash droughts under varying vegetation conditions remains poorly understood. Here we investigate the ecosystem response to the speed of flash drought onset for different plant functional types, considering the decline rate of root-zone soil moisture and standardized gross primary productivity anomaly. Our findings reveal a significant increase of approximately 10% in the proportion of 1- and 2-pentad (5 and 10 days) onset flash droughts leading to negative standardized gross primary productivity anomalies during 2001–2018. Furthermore, while standardized gross primary productivity anomalies decline at higher rates, they do not promptly respond on a shorter timescale to faster-onset flash droughts compared to slower-onset flash droughts. Vegetation types with shallower root systems exhibit higher sensitivities to faster-onset flash droughts, suggesting an escalating threat to terrestrial ecosystems in a changing climate.

Flash droughts, characterized by their rapid onset, are occurring more frequently, posing increasingly severe global risks<sup>1–7</sup>. Rapid soil moisture (SM) depletion is crucial in capturing the onset of flash droughts, and it also signifies later drought phases<sup>6,8–12</sup>. SM significantly influences ecosystem productivity and agricultural productivity under a warming climate<sup>13–16</sup>. Thus, flash droughts pose a serious threat to terrestrial ecosystems and agriculture<sup>17–20</sup>. However, there is currently a lack of assessment of ecosystem responses to flash droughts, particularly in terms of the response characteristics identified by the root-zone SM, which is more relevant to vegetation productivity<sup>14</sup>. Additionally, flash droughts are occurring more rapidly and with higher rates of intensification<sup>2,9,21,22</sup>, highlighting the need to examine ecosystem productivity responses to the decline rate of the root-zone SM during the onset of flash droughts.

The response of vegetation to flash droughts has been investigated worldwide; however, most research focuses on limited areas, such as flux tower sites<sup>23,24</sup>, specific basins<sup>25,26</sup>, or individual countries<sup>19,27–31</sup>. For example, a prior study examined the changes in ecosystem variables in response to flash droughts on a global scale, primarily considering climate conditions. However, the understanding of diverse plant functional type dynamics with varying root depths during flash droughts and the impact of secondary underlying features such as soil texture remains poorly understood<sup>32</sup>. Furthermore, less than 15% of flash drought studies are global, with only about ten studies using root-zone soil moisture<sup>2,9,11,33–36</sup>. A global assessment of ecosystem response time, based on the global Vegetation Health Index

(VHI), was conducted using surface soil moisture from NASA's Soil Moisture Active Passive<sup>37</sup> (SMAP) mission. However, more detailed characteristics, such as the rate of reduction in ecosystem productivity during flash drought events, remain unclear. Moreover, few studies investigate ecosystem productivity sensitivity to the rapid onset of flash droughts and their underlying mechanisms. Meteorological factors, including temperature, humidity, and monsoons, can influence the ecosystem response to flash droughts<sup>19,24,28</sup>, potentially impacting productivity across different climatic and vegetation regions. A comprehensive understanding of global ecosystem responses to the accelerated flash drought onset is crucial for elucidating spatial variations in flash drought impacts across plant functional types and climatic regions.

The rapid decline in gross primary production (GPP) during flash droughts can weaken ecosystem resilience and may surpass ecosystems tolerance thresholds, potentially leading to widespread mortality as per the carbon starvation hypothesis<sup>38,39</sup>. Consequently, the transition of GPP anomalies from positive to negative values during flash droughts signals the onset of an ecological response. Despite acknowledging the swift decrease in vegetation productivity during flash droughts, the timing and severity of ecosystem responses to accelerated flash droughts remain unclear. The development of plant activity is significantly correlated with the root-zone soil moisture, while different soil moisture regimes under varying drought onset mechanisms have contrasting impacts on ecological responses<sup>40</sup>. It is unclear whether the faster-developing flash droughts could result in more

<sup>1</sup>Department of Land Surveying and Geo-Informatics, The Hong Kong Polytechnic University, Hong Kong SAR, China. <sup>2</sup>Research Institute for Land and Space, The Hong Kong Polytechnic University, Hong Kong SAR, China. <sup>3</sup>Hong Kong Observatory, Hong Kong SAR, China. <sup>4</sup>Department of Geological Sciences, The John A. and Katherine G. Jackson School of Geosciences, University of Texas at Austin, Austin, TX, 78712, USA. ✉e-mail: [shuo.s.wang@polyu.edu.hk](mailto:shuo.s.wang@polyu.edu.hk)

severe productivity declines. Moreover, few studies investigate the drivers of ecosystem responses to the speed of flash drought onset.

To comprehensively assess and deeply analyze ecosystem responses to accelerated flash droughts, we thoroughly examine the relationship between flash drought intensification rates and the reduction in standardized gross primary productivity anomaly (saGPP). Specifically, we identify spatial saGPP response patterns to various flash drought onset timescales and unveil the sensitivities of saGPP to the faster-onset flash droughts across different plant functional types from 2001 to 2018. This study aims to illuminate the characteristics of ecosystem responses during flash droughts with varying intensification rates and to explore potential drivers of ecosystem productivity sensitivity to the speed of flash drought onset. By doing so, it provides valuable insights into ecosystem dynamics in the face of accelerated flash droughts, aiding in ecological risk assessment and prediction in a changing climate.

## Results

### Evaluation of saGPP responses to flash droughts at different onset times

Using five datasets (GLEAM, MERRA2, and three NASA GLDAS-2 datasets: Noah, VIC, and CLSM), we quantified the global percentage of flash droughts that resulted in negative saGPP from 2001 to 2018. Supplementary Fig. 1 demonstrates that saGPP responses have occurred across nearly all global land areas experiencing flash droughts in the five datasets. For each grid cell, we calculated the response ratio by dividing the number of flash drought events with negative saGPP responses by the total number of flash droughts. The global mean ratios across all grid cells are above 85%, indicating a high risk of damage to ecosystems. We utilized the Mann-Kendall statistic to examine the temporal dynamics of the response ratio on an annual timescale. We find that the percentage of flash droughts that result in negative saGPP relative to all flash droughts shows a significant ( $P < 0.01$ ) increasing trend globally (Supplementary Fig. 2). More importantly, the magnitude of the estimated slope suggests an increase of 9.19–11.08% in the percentage of 1- and 2-pentad onset flash drought-induced negative saGPP events, at a rate more than twice that of 1- and 2-pentad onset flash droughts (Supplementary Fig. 2). This indicates that faster-onset flash droughts have increased the frequency of flash drought-induced negative saGPP events.

To conduct a comprehensive assessment of the saGPP responses to flash droughts at different onset times, we divided flash droughts into five types according to the longest possible onset development phase, which includes 1, 2, 3, 4, and 5 pentads<sup>9</sup>. We find that 49.16–65.66% of saGPP responses to flash droughts developed in 1–2 pentads, which are the significant components of flash drought-induced saGPP decline events (Supplementary Fig. 3). We further investigated the annual evolution of the saGPP responses to flash droughts at different onset times (Fig. 1; Supplementary Fig. 4). The trend and the number of flash drought-induced saGPP decline events derived from three GLDAS models are highly consistent and align well with each other. GLEAM and MERRA-2 show the same significant increase in the proportion of saGPP responses to 1-pentad onset flash droughts, which are the fastest-onset flash droughts (Fig. 1a, Supplementary Fig. 4). Despite using different reanalysis datasets, the results consistently show an increasing trend in the proportion of saGPP responses to accelerated flash droughts, particularly for the fastest onset flash droughts that intensified within 1 pentad across all five datasets. Generally, the proportion of saGPP responses to 1-pentad onset flash droughts shows a statistically significant ( $P < 0.01$ ) increase at an annual rate of 0.11–0.27%. In contrast, the proportions of saGPP responses to flash droughts developing in 3, 4, and 5 pentads significantly decrease with an annual decline of 0.06–0.14%, 0.14–0.18%, and 0.09–0.11%, respectively (Fig. 1a, Supplementary Fig. 4). Furthermore, the faster-developing flash droughts lead to a higher increasing rate of the response ratio, implying that terrestrial ecosystems are at greater risk from accelerated flash droughts (Supplementary Fig. 5).

To advance our understanding of saGPP response characteristics, we divided the world into 21 regions for a comprehensive regional analysis of

the response ratio, excluding the Sahara due to the absence of valid GPP data (Supplementary Table 1). This analysis utilized an ensemble of results from five datasets. Similar trends were observed in most sub-regions, with the most significant increase in the response ratio of faster-onset flash droughts occurring in Southern Africa, Western Africa and Eastern Africa (Fig. 1b). Seven regions exhibit significant increases in the percentage of 1- and 2-pentad onset flash droughts that result in negative saGPP. These regions include ALA, AUS, EAF, NEU, SAF, SAS, and WAF. This indicates that a greater number of saGPP decline events occurred during the faster-onset flash droughts across most regions. To fully grasp the intricate relationship between the GPP reduction and the rapid SM depletion, it is imperative to consider the significant threat posed to ecosystems by the faster-onset flash droughts across various climate regions.

### Relationships between the SM decline and the saGPP reduction

It is widely acknowledged that SM plays a crucial role in driving GPP<sup>14,31,41</sup>. This relationship is also a defining feature of flash droughts, characterized by their rapid onset and rapid intensification. Therefore, we conducted a sensitivity assessment of saGPP reduction rates based on flash drought onset timescales. Generally, a greater absolute value indicates a faster decline in saGPP. Significant variations were observed between flash droughts with different onset times (Fig. 2a), indicating the heightened sensitivity of saGPP decline rates in response to flash droughts that develop more rapidly.

To explore the intricate relationship between the GPP response and the rapid onset phase of flash droughts, we conducted an in-depth assessment of the relative sensitivity of saGPP to the intensification rate. We categorized the intensification rate based on the percentile of SM decline per pentad. Using a regression model, we examined the relationship between the saGPP reduction rate and the specific depletion rate of SM percentiles. Like Fig. 2a, we identified a statistically significant cubic curve for the saGPP reduction rate ( $R^2 = 0.847$ ,  $P < 0.0001$ ), indicating that GPP is more sensitive to flash droughts with higher intensification rates (Fig. 2b).

### Causal relationships between the SM decline and the GPP response

The uWUE links carbon and water vapor fluxes in soil–plant–atmosphere interactions. Different responses of uWUE reflect the varying sensitivities of ecosystem processes to changes in hydro-climatic conditions<sup>31,42</sup>. Therefore, to perform an attribution analysis on the sensitivity of GPP responses to the faster-onset flash droughts, we compared the mean anomalies of uWUE and meteorological factors during the onset stage between flash droughts with and without GPP response at different onset times. Generally, flash droughts with the 1–2 pentad onset time exhibit significantly higher anomalies in evapotranspiration (ET), vapor pressure deficit (VPD), latent heat (LH), downward shortwave radiation (SW), and temperature (T) compared to flash droughts developing in 3–5 pentads (Supplementary Fig. 6). These factors tend to drive a rapid decline in GPP. Additionally, ET and LH display positive mean anomalies for flash droughts with the GPP response and negative mean anomalies for those without the GPP response. Importantly, we find that the ensemble mean values of uWUE anomalies during the onset stage of flash droughts with a GPP response are much lower than those without a GPP response, based on the five datasets (Fig. 3a). Furthermore, our analysis reveals that negative uWUE anomalies are associated with 1- and 2-pentad onset flash droughts, while positive uWUE anomalies accompany flash droughts developing in 3, 4, and 5 pentads. This suggests different adaptive adjustments in ecosystem physiology in response to the varying rates of SM decline, resulting in different sensitivities of GPP to the speed of flash drought onset.

SM plays a pivotal role in controlling variations in GPP and ET in water-limited ecosystems. This, in turn, affects the variation in underlying uWUE. Moreover, factors such as ET, VPD, and LH that are associated with GPP are identified as the primary influences on uWUE in soil–plant–atmosphere interactions<sup>43,44</sup>. Therefore, it is imperative to explore the contribution of carbon and water coupling chains in these

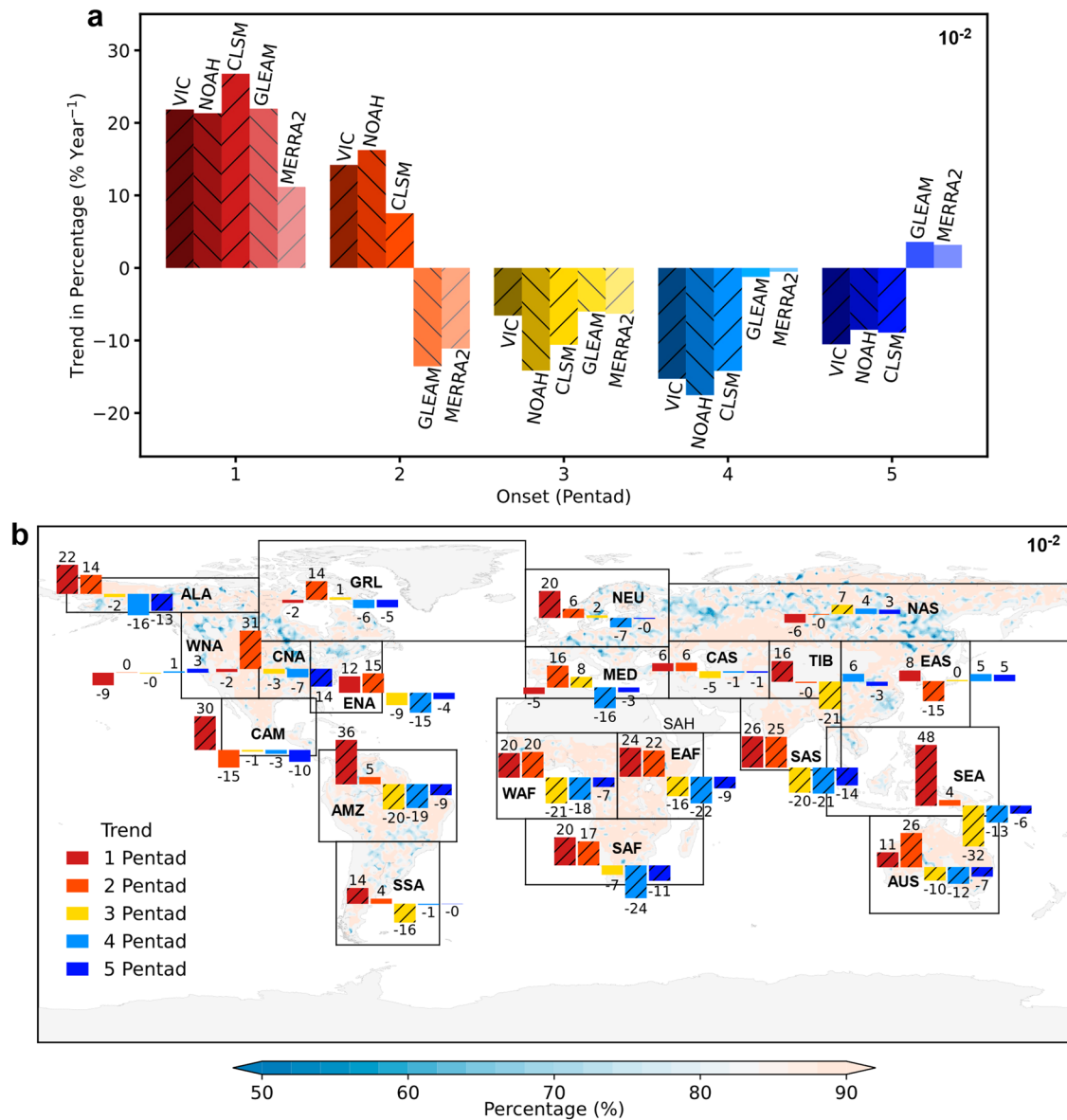


**Fig. 1 | Temporal dynamics of the response ratio of flash droughts at different onset times. a** Trends of the percentage of 1-, 2-, 3-, 4-, and 5-pentad onset flash droughts resulting in negative saGPP relative to all flash droughts with saGPP responses across five different datasets. **b** Temporal trends of the percentage of different onset flash droughts resulting in negative saGPP relative to all flash droughts

with saGPP responses across 21 regions, based on the mean results from GLEAM, MERRA2, Noah, CLSM, and VIC, evaluated by the magnitude of Sen’s slope. Bars with slashes indicate trends that are statistically significant at the 0.05 level. The linear annual trends are estimated using Sen’s slope estimator, and statistical significance is determined by the Mann-Kendall test for the study period (2001–2018).

interactions to understand the sensitivity of GPP to the faster-onset flash droughts. To investigate these mechanisms, we conducted a causality analysis using the convergent cross-mapping algorithm to detect causal relationships within the SM–meteorological factors–GPP transitive chains<sup>45,46</sup>. To comprehend the reasons for the increased sensitivity of GPP to the faster-onset flash droughts, we analyzed the dynamics of meteorological factors between the period prior to the flash drought onset (one pentad before) and the onset stage of flash droughts, as well as the decline rate of the root-zone SM and saGPP. Generally, SM dynamics drive changes in latent heat flux and evapotranspiration dynamics, which subsequently affect productivity dynamics. This is evident from the significant causal relationships between the SM decline rate and changes in meteorological conditions (Fig. 3b), as well as the significant causal relationships between changes in meteorological conditions and the saGPP decline rate (Fig. 3c). Our findings suggest that, among various meteorological factors, both ET and LH chains are significantly correlated with GPP sensitivity to the SM decline. This implies that the carbon and water coupling chains, particularly the changes

in ET and LH within the chains, may be the dominant transitive processes responsible for the increased sensitivity of ecosystem responses to accelerated flash droughts (Supplementary Figs. 7, 8).

**Differences in ecosystem plant functional types in response to flash drought**

Plant functional types (PFTs) categorize species based on their structural, physiological, and/or phenological characteristics in response to environmental disturbance<sup>47–49</sup>. As a result, the response ratio and sensitivity of saGPP decline to flash droughts may vary among PFTs<sup>50,51</sup>. Additionally, plant root systems play a crucial role in ecosystem response to dryness stress<sup>52,53</sup>. We assessed the dependence of saGPP response ratios and sensitivities on PFTs (Supplementary Tables 2 and 3). Generally, we observed distinct response characteristics of ecosystem productivity to flash droughts across different PFTs based on the root depth. Specifically, shallower root depths are usually found in grasslands, herbs, and savannas, while deeper roots are in large, broadleaf forests<sup>13,54,55</sup>.

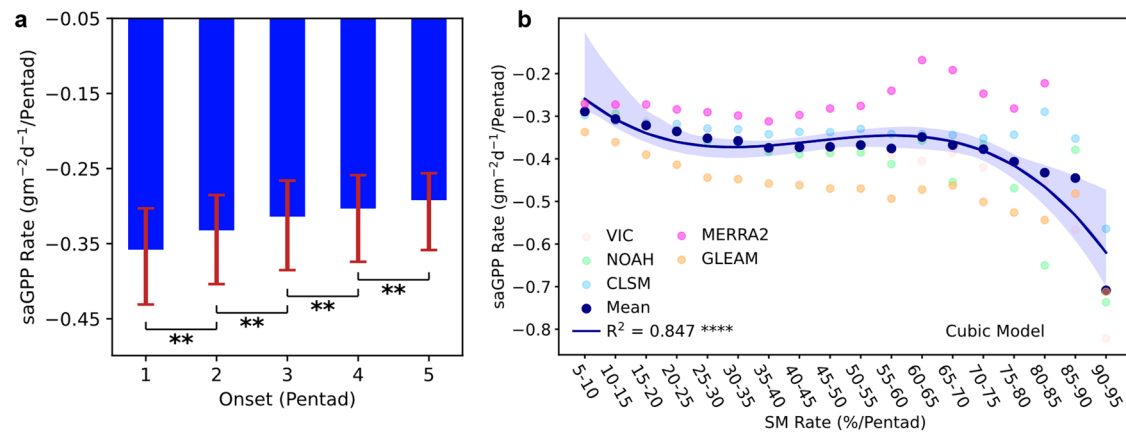


**Fig. 2 | Relationship between the saGPP reduction and the SM decline.** **a** Variation in saGPP reduction rates across different timescales of flash droughts onset phases. The Mann–Whitney U test was employed to determine the significant difference ( $P < 0.01$ ) between flash drought onset timescales. The red lines above each bar indicate the range of uncertainty across five different datasets. **b** A cubic relationship

between saGPP reduction rates and intensification rates of flash drought onset phase. The navy dots represent the mean value of saGPP rates in the corresponding SM depletion rate category from the five datasets. The blue ribbon represents the 95% confidence interval, reflecting the structural uncertainty of the cubic spline models.

The response ratio showed a significantly increasing trend in evergreen broadleaf forest (EBF), evergreen needleleaf forest (ENF), mixed forest (MF), and grasslands (GRA) (Supplementary Fig. 9). Moreover, there was a notable increase in the response ratio of croplands (CRO), savannas (SAV), shrublands classes (SHB), GRA, EBF, and ENF to 1- and 2-pentad onset flash droughts. This suggests that evergreen forests and grasslands may face a higher risk of flash droughts, especially those with a 1-2 pentad onset (Supplementary Fig. 10). In contrast, most ecosystems with shallower rooting zones<sup>13,54</sup> only experienced more significant threats posed by the faster-onset flash droughts.

Interestingly, similar differences were also observed in sensitivity. The variation in sensitivity between different onset flash droughts was statistically significant in SAV, CRO, GRA, EBF, and SHB (Fig. 4a–e). In contrast, deciduous and mixed forests did not exhibit significant differences (Fig. 4f–i). This suggests a greater sensitivity of GPP for shallow-rooted plants than deep-rooted plants when flash droughts develop over a shorter timescale, especially for SAV.

To investigate the response of vegetation to flash drought in more detail, we also assessed the uWUE across different PFTs, which is closely related to physiological characteristics<sup>56,57</sup>. Changes in various physiological and structural characteristics of vegetation due to flash droughts may result in different uWUE changes, indicating that ecosystems with distinct physiological and structural characteristics may have diverse responses to different flash drought onset conditions. This is particularly true for ecosystems employing different strategies to cope with flash drought stress, as vegetation with unique physiological and structural characteristics may respond differently<sup>58,59</sup>. Thus, we integrated the mean uWUE anomaly during the flash drought onset stage of different PFTs with the saGPP response sensitivities between flash droughts with and without saGPP responses (Supplementary Fig. 11). We find that for the PFTs that are more sensitive to accelerated flash droughts, the uWUE anomalies of flash droughts with saGPP responses show a significant reduction compared to those without saGPP responses. This indicates considerable adaptive adjustments in ecosystem physiology during the rapid decline in SM. Interestingly, forests tend to experience negative uWUE anomalies, implying their contrasting physiological adjustments compared to flash droughts without a response.

## Discussion

While the ecological impacts of flash droughts have garnered considerable attention, a global assessment of how terrestrial ecosystems respond to the rapid onset of flash droughts across various PFTs remains unclear. In this study, we conducted a comprehensive analysis to quantify both the overall

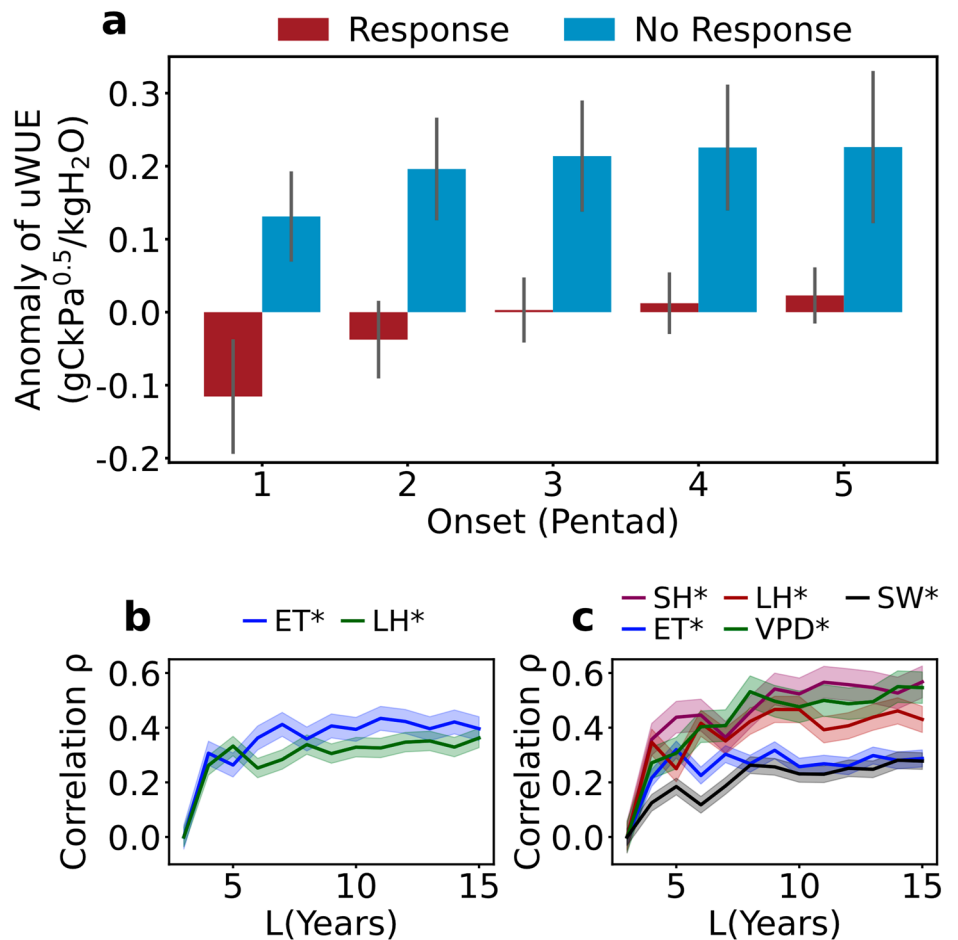
and diverse vegetation response ratios and sensitivities of terrestrial ecosystem productivity to the SM decline rate during the onset of flash droughts. By examining the relationship between the saGPP reduction rate and the intensification rate of flash droughts, our study provides a deeper understanding of the ecological risks associated with accelerated flash droughts. Our findings reveal that the faster-onset flash droughts can result in a higher response ratio and a more rapid decline in saGPP, indicating that terrestrial ecosystem productivity is more sensitive to accelerated flash droughts.

It is widely acknowledged that flash droughts develop due to increased evaporative demand and precipitation deficits<sup>17</sup>. Two main methodologies have been used to assess flash droughts. The first approach relies upon the evaporative stress ratio (ESR), which combines evapotranspiration to investigate climatological characteristics<sup>60</sup>. Pentad-mean soil moisture has also been used to examine flash droughts based on declining rates<sup>21</sup>. Additionally, we find that Africa and Asia experience a greater number of saGPP decline events during the faster-onset flash droughts, where flash droughts calculated by soil moisture occur frequently and have a significant impact on agriculture<sup>61–63</sup>.

We observed a significant increase in the percentage of flash droughts at 1- and 2-pentad onset that resulted in negative saGPP (Supplementary Fig. 2). Conversely, there was a notable decrease in the percentage of flash droughts occurring in 3–5 pentads that resulted in negative saGPP. The primary explanation for the increased response ratio is the occurrence of the 1- and 2-pentad onset flash droughts with saGPP responses (Supplementary Fig. 2). Therefore, it is the faster-onset flash droughts, influenced by a warming climate, that have made GPP more sensitive. In addition, seven sub-regions show significant increases in response ratios of faster-onset flash droughts, which are largely concentrated in areas with a high proportion of faster-onset flash droughts accompanied by GPP responses (Supplementary Fig. 3).

It should be noted that previous studies have overlooked the subsequent effects of flash droughts<sup>24</sup>. By comparing the timing of minimum saGPP occurrence and the duration for flash drought events across all grid points, we improve the understanding of these subsequent effects. We find that less than 10% of events reach the minimum saGPP after the end of flash droughts, with an average lag time of less than 2 pentads between the later occurrence of minimum saGPP and the end of flash droughts (Supplementary Fig. 12). Therefore, we identified the minimum saGPP at longer timescales, beyond just the duration of flash droughts, to account for the legacy effects of flash droughts on ecosystems. Furthermore, to advance our understanding of the impacts of accelerated flash droughts on ecosystem response characteristics, we examined the response time, the timing of

**Fig. 3 | Detection of uWUE and potential meteorological influences on the sensitivity of GPP to faster-onset flash droughts.** **a** Comparison of uWUE anomalies during the onset stage between flash droughts with and without GPP responses at different onset times. The gray lines above each bar represent the range of uncertainty across five datasets. **b** Significant causal relationships between SM and meteorological factors. **c** Significant causal relationships between meteorological factors and GPP reduction. An asterisk denotes a significant causal connection ( $P < 0.05$ ) identified through convergent cross mapping. The  $x$  axis represents the time-series length ( $L$ , years). The  $y$  axis represents the cross-map skill measured by correlation coefficient ( $\rho$ ). The shaded regions indicate the 90% confidence interval. The results are based on the mean from five datasets for ET and VPD, while other factors are from four datasets except GLEAM.



minimum saGPP occurrence, and the magnitude of minimum saGPP across different onset timescales. We find that similar response times and minimum saGPP values are consistent across different onset times, while flash droughts with shorter onset timescales lead to an earlier occurrence of minimum saGPP (Supplementary Fig. 13). Thus, accelerated flash droughts do not lead to shorter timing of ecosystem responses. Additionally, faster-developing flash droughts do not result in significantly more severe productivity declines.

To further explore the response characteristics, we conducted a sensitivity analysis comparing ecosystem productivity responses to flash droughts identified by root-zone SM and surface SM. We find that GPP consistently shows sensitivity to the fastest-onset flash droughts identified by surface SM (Supplementary Figs. 14, 15) and responds to these droughts on a consistently short timescale (Supplementary Fig. 16). However, using root-zone SM can result in significantly more severe productivity declines and longer-lasting effects (Supplementary Fig. 16). Flash droughts identified by surface SM may not fully reflect ecosystem responses, as ecosystems with deeper root systems, such as forests, can absorb deeper groundwater and mitigate dry conditions. Therefore, we use root-zone SM data from the five datasets to consider the more direct impacts to ecosystem root systems compared to surface SM.

At the ecosystem scale, we also explored the response time, the timing of minimum saGPP occurrence and the magnitude of minimum saGPP for different PFTs. We find that forests tend to respond and reach their peak at longer timescales, indicating a lower risk (Supplementary Fig. 17). Additionally, needle-leaf forests, SAV, and SHB tend to exhibit lower minimum saGPP values, signifying more substantial impacts from flash droughts. Our study also highlights contrasting patterns of ecosystem productivity sensitivity on faster-onset flash droughts between shallow-rooted and deep-rooted PFTs, providing supplementary insights into the sensitivity of

different ecosystems to flash droughts at various onset times. Generally, we observed significant differences in temporal dynamics of the response ratio and saGPP decline rates based on flash drought onset timescales across PFTs with varying root depths, aligning with recent findings that suggest shallower-rooted plants, particularly savannas and grassland, are more sensitive to early stages of dryness<sup>24,64–66</sup>. No significant differences were observed in most forest ecosystems, which tended to have deeper roots. In contrast, EBF showed high sensitivity to the faster-onset flash droughts. By comparing the spatial distributions of vegetation in relation to latitude (Supplementary Fig. 18), we find that the less sensitive types are predominantly located in the northern high latitude where response ratios are low (Supplementary Fig. 1), while the more sensitive types, especially EBF, are distributed from 20° S to 20° N. This distribution may contribute to a higher sensitivity compared to other forest types. Furthermore, the coexistence of vegetation with soil and climate could significantly impact ecosystem responses to flash droughts. The same plant within different soils may behave differently under similar drought-inducing meteorological conditions<sup>55,67</sup>. The GLDAS soil texture data for Noah, based on the Food and Agriculture Organization (FAO), was used to identify different soils, indicating the impact of secondary underlying features on the response of the same plant functional type to flash droughts (Supplementary Fig. 19, Supplementary Tables 4 and 5). We find that the proportions of different soil texture classes vary across different PFTs. For instance, PFTs such as SAV and EBF are distributed more within loamy soils of moderately fine texture, while other PFTs are distributed more within loamy soils of medium texture (Supplementary Fig. 20). Additionally, the sensitivities of saGPP reduction rates to flash drought onset timescales differ for the same PFT within different soils. Generally, the soil texture class with more vegetation distribution may exhibit similarly higher sensitivity for the same plant species. However, CRO shows high sensitivity to different onset flash

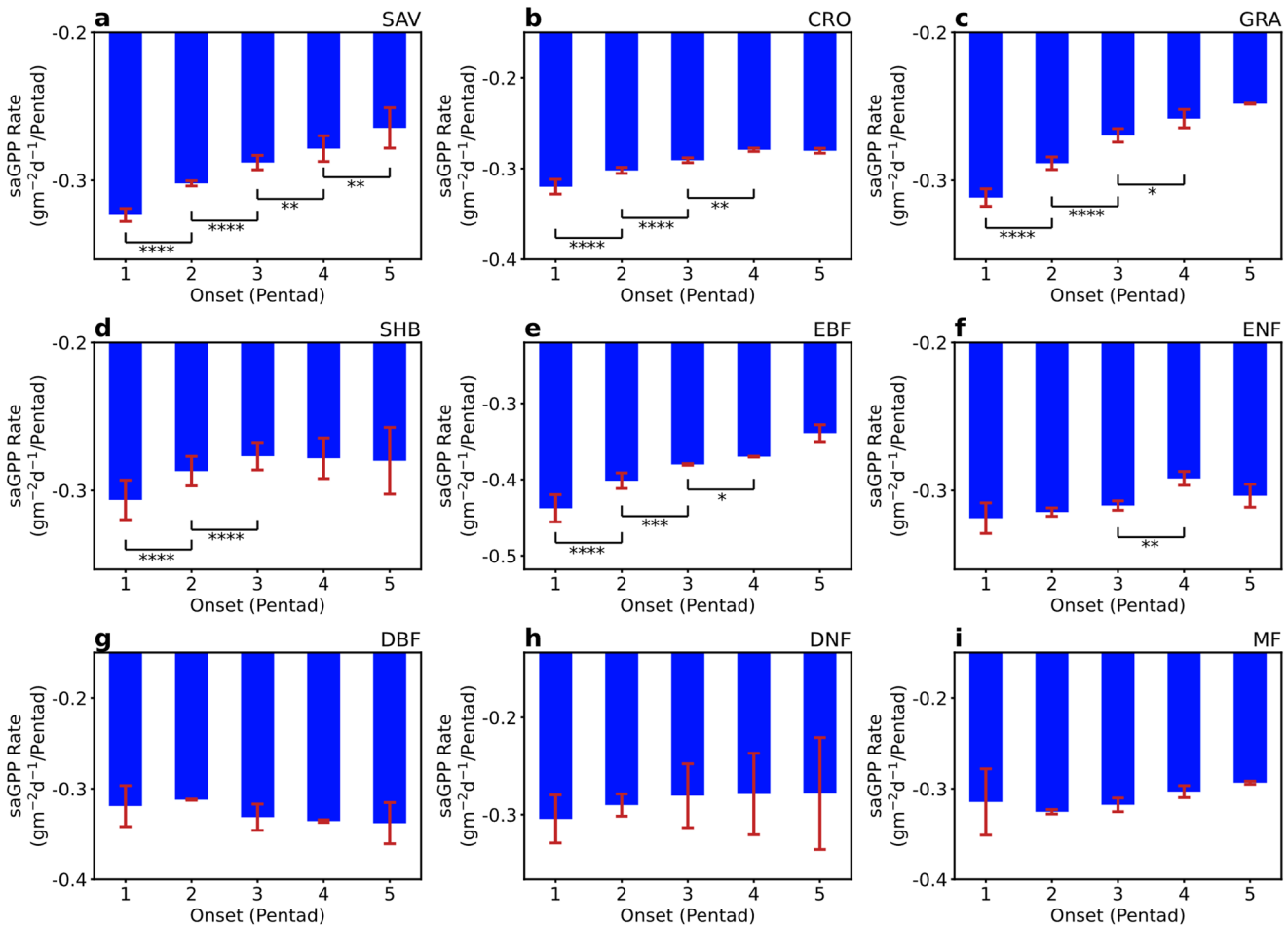


**Fig. 4 | The sensitivity of saGPP reduction rate to flash droughts onset timescales for different plant functional types (PFTs).** a–i Variation in saGPP reduction rates across different timescales of flash drought onset phases for the nine selected PFTs. The red lines above each bar indicate the range of uncertainty across the Noah and VIC datasets. The significance testing follows the same criteria as in Fig. 2a. SAV,

CRO, GRA, SHB, EBF, ENF, DBF, DNF, and MF represent savannas, croplands, grasslands, shrublands classes (closed shrublands and open shrublands), evergreen broadleaf forest, evergreen needleleaf forest, deciduous broadleaf forest, deciduous needleleaf forest, and mixed forest, respectively.

droughts across all five soil textures used in this study (Supplementary Figs. 21–29).

Our study reveals that the magnitude of the rate of saGPP reduction in response to flash droughts is influenced by the decline rate of SM during the onset phase of flash droughts and varies among PFTs. Particularly, we observe a significant increase in the percentage of faster-onset flash drought events associated by ecosystem responses. Importantly, we emphasize that the faster-onset flash droughts lead to a more rapid saGPP decline rate. The rate of saGPP reduction varies across PFTs, highlighting the potential of saGPP to monitor the rapid response characteristics of different ecosystems to flash droughts. We also underscore the sensitivity of ecosystems to flash droughts, particularly their vulnerability to the faster-onset flash droughts. Flash droughts are expected to come on faster in most global regions<sup>9,21</sup>. Therefore, we need to pay more attention to ecosystems that are more sensitive to faster-onset flash droughts and develop corresponding measures for different plant types. According to our study, the exchange of carbon and water vapor fluxes in soil–plant–atmosphere interactions via stomata (low uWUE) contributes to ecosystem response sensitivity. Changes in ET and LH anomalies are likely to trigger a rapid reduction of saGPP during the faster-onset flash droughts. Negative uWUE anomalies indicate a threat to ecosystem functioning posed by the faster-onset flash droughts. Moreover, the varying response of uWUE to flash drought may result from different sensitivities of ecosystem processes to changes in SM conditions. This underscores the significance of understanding the response of carbon and water fluxes, as well as the coupling between them, to flash droughts. It is

worth noting that our study primarily focuses on the soil–plant–atmosphere interactions and aims to confirm that the coupling chains of SM – LH and evapotranspiration–GPP contribute to the sensitivity of ecosystem responses to flash droughts. This implies that the exchanges of carbon and water vapor fluxes may be one of the reasons for the different sensitivity.

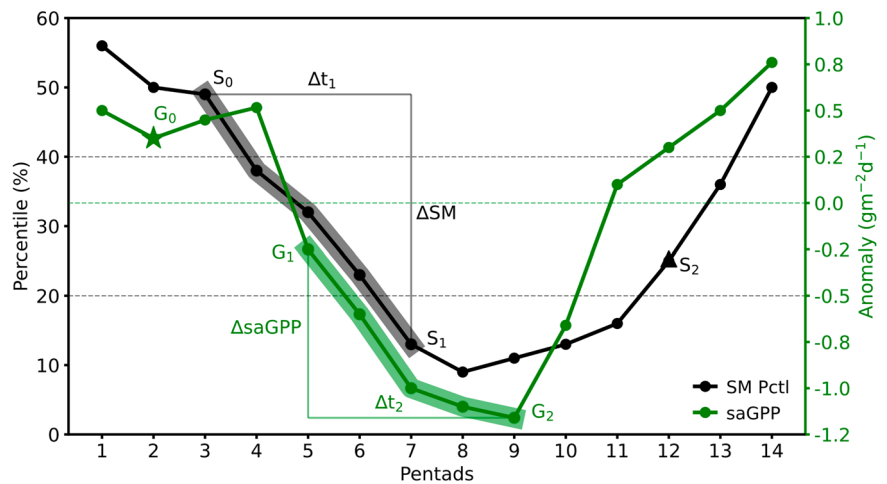
Collectively, our findings suggest that accelerated flash droughts can pose even more serious threats to terrestrial ecosystem productivity and provide a more comprehensive understanding of diverse ecosystem dynamics in response to flash droughts and the underlying factors affecting the response sensitivity. Understanding the relationship between the GPP response and the rapid intensification rate which is the most important characteristic of flash droughts can provide valuable insights to inform policymakers and stakeholders about the early warning of serious threats to vegetation vulnerability posed by accelerated flash droughts. To advance our understanding of ecosystem responses to flash droughts, more research efforts should be dedicated to investigating the terrestrial carbon–water coupling across different climates and ecosystem regions. Assessing the contribution of stomatal conductance to different response sensitivities of flash droughts is also essential in future studies.

## Methods

### Datasets

In this study, daily evapotranspiration (ET), latent heat (LH), sensible heat (SH), downward shortwave radiation (SW) and soil temperature (ST) were obtained from three NASA GLDAS-2 (Global Land Data Assimilation

**Fig. 5 | Schematic representation of the method used to identify ecosystem response during a flash drought event.** As for flash droughts, SM decreases from above the 40th percentile ( $S_0$ ) to below the 20th percentile ( $S_1$ ) with an average decline rate of no less than the 5th percentile for each pentad, and SM below the 20th percentile should last for no less than 3 pentads. Ecosystem response to flash droughts is determined as the first occurrence of saGPP less than zero ( $G_1$ ) during the whole duration of flash droughts from  $S_0$  to  $S_2$ , and saGPP before (one pentad prior to flash drought onset point ( $S_0$ )) should be greater than zero ( $G_0$ ). saGPP decreases from the first negative response ( $G_1$ ) to its minimum value ( $G_2$ ). It should be noted that saGPP may reach the peak ( $G_2$ ) later than flash drought termination ( $S_2$ ). The black solid line represents the 5-day mean SM percentile for a grid point, and the black shading line indicates the onset phase of a flash drought event. The green solid line represents the saGPP at one pentad for a grid point, and the green shading line indicates the development of saGPP response.



System Version 2) models<sup>68,69</sup>, including Noah<sup>70,71</sup>, Catchment land surface models (CLSM)<sup>72</sup>, and the Variable Infiltration Capacity (VIC) model<sup>73,74</sup>. Daily root-zone soil moisture (SM) was obtained from the Global Land Evaporation Amsterdam Model (GLEAM) (<https://www.gleam.eu/>), the Modern-Era Retrospective Analysis for Research and Applications, version 2 (MERRA-2) (<https://disc.gsfc.nasa.gov>), Noah, CLSM, and VIC datasets. The parameters selected for root-zone soil moisture are SMroot, GWET-ROOT, RootMoist\_inst, SoilMoist\_RZ\_tavg, RootMoist\_inst for GLEAM, MERRA-2, Noah, CLSM, and VIC, respectively. Noah and VIC determine root-zone depth based on vegetation types. CLSM does not have explicit vertical levels for soil moisture and uses a uniform depth of 100 cm for the root zone. The root-zone depth for GLEAM comprises three model layers for tall vegetation (0–10, 10–100, and 100–250 cm), two for low vegetation (0–10, 10–100 cm), and one for bare soil (0–10 cm)<sup>75</sup>. Daily ET, LH, SH, SW, and ST were obtained from MERRA-2. Daily ET was obtained from GLEAM. Daily estimates of GPP were obtained from the MODIS GPP product FluxSat v2.0 using the FLUXNET eddy covariance tower site data and coincident satellite data<sup>65,76</sup>. We used the daily near-surface (2-m) temperature (T) and dew-point T data from the European Centre for Medium-Range Weather Forecasts (ERA5) to calculate daily vapor pressure deficit (VPD). Daily VPD was defined as the difference between saturated water vapor pressure, determined by near-surface T, and actual water vapor pressure, determined by dew-point T. Daily underlying water use efficiency (uWUE) was calculated using MODIS FluxSat GPP, ET from three GLDAS-2 models and VPD from the ERA5 dataset, considering the nonlinear relationships between GPP, VPD and ET<sup>42</sup>. All these data were aggregated to the same resolution at  $1^\circ \times 1^\circ$  and a temporal resolution of pentads for 2001–2018. The Global Land Data Assimilation System (GLDAS) Vegetation Class/Mask data for VIC and Noah was used to identify the plant functional types<sup>77</sup>.

**Identification of flash droughts and ecosystem responses**

To quantify the relationship between ecosystem responses and flash droughts, we took into account the flash drought intensification rate and the rate of reduction in standardized gross primary productivity anomaly (saGPP). As for flash drought events, the pentad (5 days) indicates the root-zone SM decreasing from above the 40th percentile to below the 20th percentile, with an average decline rate of no less than the 5th percentile for each pentad. The 40th and 20th percentiles were determined throughout the same pentad for each year over the study period to enable a comparison of relative SM changes throughout the same time each year<sup>9</sup>. The root-zone SM was used to identify flash droughts as it is closely related to vegetation

dynamics. Moreover, we used the saGPP to represent the ecological impact, which could remove the influence of seasonality and ensure comparability in space. The saGPP was calculated as follows:

$$saGPP = \frac{GPP - \mu_{GPP}}{\sigma_{GPP}} \tag{1}$$

where  $\mu_{GPP}$  and  $\sigma_{GPP}$  represents mean and standard deviation of GPP, respectively, for the same pentad over the study period.

As shown in Fig. 5, we identified ecosystem responses in terms of the first occurrence of negative saGPP ( $G_1$ ) during the period from flash drought onset point ( $S_0$ ) to the end point where SM rises up to the 20th percentile again ( $S_2$ )<sup>24</sup>. Additionally, saGPP before the flash drought onset point (one pentad prior to flash drought onset point ( $S_0$ )) should be greater than zero ( $G_0$ ), indicating the flash drought impact on ecosystems. It should be noted that saGPP may reach the peak ( $G_2$ ) later than flash drought termination ( $S_2$ ), implying the potential lagged effects of flash drought. Since the rapid onset is the most important characteristic of flash droughts and the timing and intensity of saGPP response reflect flash drought-induced reduction of GPP, we calculated the intensification rate of flash droughts based on the changing percentiles of SM per pentad during the onset development phase of flash droughts, and then calculated the saGPP decline rate per pentad between the first negative point of saGPP and its minimum peak value to quantify the saGPP response during flash droughts. The response ratio of flash droughts that result in negative saGPP to the total number of flash droughts indicates a threat to ecosystem posed by flash droughts. The response time and the occurrence time of minimum saGPP are determined as the lag time between the flash drought onset point and the first negative point of saGPP ( $G_1 - S_0$ ) and the lag time between the flash drought onset point and the minimum saGPP occurrence ( $G_2 - S_0$ ), respectively.

**Detection of temporal trends**

The Mann-Kendall (M-K) method is a non-parametric test commonly used to examine whether there is a monotonic trend in the time series of a specific variable<sup>78,79</sup>. Positive values of standardized test statistic  $Z_{MK}$  indicate an increasing trend, while negative  $Z_{MK}$  values suggest a decreasing trend. The advantage of this method lies in its independence from specific statistical distribution requirements, making it robust against outliers. This method can effectively characterize the trends in time series data. In this study, the M-K trend analysis was performed to examine the trend in response ratio on global, climate region, and

vegetation regime scales. For a given time series  $(x_1, \dots, x_n)$ , the test statistic  $Z_{MK}$  was calculated as follows:

$$S = \sum_{i=1}^{n-1} \sum_{j=i+1}^n \text{sign}(x_j - x_i) \quad (2)$$

$$\text{sign}(x_j - x_i) = \begin{cases} +1, & x_j > x_i \\ 0, & x_j = x_i \\ -1, & x_j < x_i \end{cases} \quad (3)$$

$$\text{Var}(S) = \frac{1}{18} \left[ n(n-1)(2n+5) - \sum_p t_p(t_p-1)(2t_p+5) \right] \quad (4)$$

$$Z_{MK} = \begin{cases} \frac{S-1}{\sqrt{\text{Var}(S)}} & \text{if } S > 0 \\ 0 & \text{if } S = 0 \\ \frac{S+1}{\sqrt{\text{Var}(S)}} & \text{if } S < 0 \end{cases} \quad (5)$$

where  $n$  represents the length of the time series.  $x_i$  and  $x_j$  are the sequential data in the time series.  $t_p$  denotes the number of ties for the  $p_{th}$  value.

### Detection of causal relationships

Convergent cross mapping is a powerful methodological approach used to distinguish causality from spurious correlations in time series data of non-linear dynamical systems, overcoming the inherent limitations of inferring causality through simple correlation<sup>80</sup>. This method assesses causation by examining the extent to which the historical record of the affected variable  $Y$  (or its proxies) can reliably estimate the states of a causal variable  $X$ . If variable  $X$  is influencing  $Y$ , the estimation skill or predictability of cross-mapping improves with the length ( $L$ ) of time series, as indicated by the increasing strength of correlation ( $\rho$ ) between observed and predicted values. This enhancement in cross-mapping provides grounds to infer the causal relationship between  $X$  and  $Y$ .

In this study, the convergent cross mapping analysis was implemented using the rEDM package<sup>81</sup> provided by the authors of the extended CCM. We analyzed dynamical systems with the optimal embedding dimension estimated by simplex projection, based on yearly data for the study period.

### Data availability

All data in this study are publicly available. The three NASA GLDAS-2 datasets are available at <https://disc.sci.gsfc.nasa.gov/datasets?keywords=GLDAS>. The ERA5 dataset is available at <https://www.ecmwf.int/en/forecasts/datasets/reanalysis-datasets/era5>. The GLEAM dataset is available at <https://www.gleam.eu/>. The MERRA-2 dataset is available at <https://disc.gsfc.nasa.gov>. The Global MODIS and FLUXNET-derived Daily GPP V2 FluxSat 2.0 dataset is available at <https://doi.org/10.3334/ORNLDAAC/1835>. The GLDAS Vegetation Class/Mask data for VIC and Noah are available at <https://ldas.gsfc.nasa.gov/gldas/vegetation-class-mask>. The GLDAS Soil Texture Class data for Noah is available at <https://ldas.gsfc.nasa.gov/gldas/soils>. The saGPP data of pentads for 2001–2019 and source data for figures are available at <https://doi.org/10.5281/zenodo.10216541>.

### Code availability

Analysis and figure generation were performed using R and Python, and the codes are available from the corresponding author.

Received: 20 March 2024; Accepted: 9 January 2025;

Published online: 17 January 2025

### References

- Pendergrass, A. G. et al. Flash droughts present a new challenge for subseasonal-to-seasonal prediction. *Nat. Clim. Change* **10**, 191–199 (2020).
- Zeng, Z. et al. Increased risk of flash droughts with raised concurrent hot and dry extremes under global warming. *npj Clim. Atmos. Sci.* **6**, 134 (2023).
- Christian, J. I. et al. Global distribution, trends, and drivers of flash drought occurrence. *Nat. Commun.* **12**, 6330 (2021).
- Yuan, X. et al. Anthropogenic shift towards higher risk of flash drought over China. *Nat. Commun.* **10**, 4661 (2019).
- Mishra, V., Aadhar, S. & Mahto, S. S. Anthropogenic warming and intraseasonal summer monsoon variability amplify the risk of future flash droughts in India. *npj Clim. Atmos. Sci.* **4**, 1 (2021).
- Otkin, J. A. et al. Flash droughts: A review and assessment of the challenges imposed by rapid-onset droughts in the United States. *Bull. Am. Meteor. Soc.* **99**, 911–919 (2018).
- Parker, T., Gallant, A., Hobbins, M. & Hoffmann, D. Flash drought in Australia and its relationship to evaporative demand. *Environ. Res. Lett.* **16**, 064033 (2021).
- Ford, T. W. & Labosier, C. F. Meteorological conditions associated with the onset of flash drought in the Eastern United States. *Agric. For. Meteorol.* **247**, 414–423 (2017).
- Qing, Y., Wang, S., Ancell, B. C. & Yang, Z. L. Accelerating flash droughts induced by the joint influence of soil moisture depletion and atmospheric aridity. *Nat. Commun.* **13**, 1139 (2022).
- Hunt, E. D., Hubbard, K. G., Wilhite, D. A., Arkebauer, T. J. & Dutcher, A. L. The development and evaluation of a soil moisture index. *Int. J. Climatol.* **29**, 747–759 (2009).
- Mukherjee, S. & Mishra, A. K. Global flash drought analysis: uncertainties from indicators and datasets. *Earth's Future* **10**, e2022EF002660 (2022).
- Mahto, S. S. & Mishra, V. Flash drought intensification due to enhanced land-atmospheric coupling in India. *J. Climate* **37**, 5291–5307 (2024).
- Song, J. et al. A meta-analysis of 1,119 manipulative experiments on terrestrial carbon-cycling responses to global change. *Nat. Ecol. Evol.* **3**, 1309–1320 (2019).
- Stocker, B. D. et al. Drought impacts on terrestrial primary production underestimated by satellite monitoring. *Nat. Geosci.* **12**, 264–270 (2019).
- Liu, L. et al. Soil moisture dominates dryness stress on ecosystem production globally. *Nat. Commun.* **11**, 4892 (2020).
- Xu, C. et al. Increasing impacts of extreme droughts on vegetation productivity under climate change. *Nat. Clim. Change* **9**, 948–953 (2019).
- Christian, J. I. et al. Global projections of flash drought show increased risk in a warming climate. *Commun. Earth. Environ.* **4**, 165 (2023).
- Mahto, S. S. & Mishra, V. Increasing risk of simultaneous occurrence of flash drought in major global croplands. *Environ. Res. Lett.* **18**, 044044 (2023).
- Sungmin, O. & Park, S. K. Flash drought drives rapid vegetation stress in arid regions in Europe. *Environ. Res. Lett.* **18**, 014028 (2023).
- Zhang, M., Yuan, X. & Otkin, J. A. Remote sensing of the impact of flash drought events on terrestrial carbon dynamics over China. *Carbon Balance Manag* **15**, 20 (2020).
- Yuan, X. et al. A global transition to flash droughts under climate change. *Science* **380**, 187–191 (2023).
- Wang, Y. & Yuan, X. Land-atmosphere coupling speeds up flash drought onset. *Sci. Total Environ.* **851**, 158109 (2022).
- Xi, X. & Yuan, X. Significant water stress on gross primary productivity during flash droughts with hot conditions. *Agric. For. Meteorol.* **324**, 109100 (2022).
- Zhang, M. & Yuan, X. Rapid reduction in ecosystem productivity caused by flash droughts based on decade-long FLUXNET observations. *Hydrol. Earth Syst. Sci.* **24**, 5579–5593 (2020).
- Yang, L., Wang, W. & Wei, J. Assessing the response of vegetation photosynthesis to flash drought events based on a new identification framework. *Agric. For. Meteorol.* **339**, 109545 (2023).

26. Yao, T., Liu, S., Hu, S. & Mo, X. Response of vegetation ecosystems to flash drought with solar-induced chlorophyll fluorescence over the Hai River Basin, China during 2001–2019. *J. Environ. Manage.* **313**, 114947 (2022).
27. Kang, M., Hao, Y. & Choi, M. The effects of flash drought on the terrestrial ecosystem in Korea. *J. Hydrol.* **624**, 129874 (2023).
28. Poonia, V., Kumar Goyal, M., Jha, S. & Dubey, S. Terrestrial ecosystem response to flash droughts over India. *J. Hydrol.* **605**, 127402 (2022).
29. Jin, C. et al. The 2012 Flash Drought Threatened US Midwest Agroecosystems. *Chin. Geogr. Sci.* **29**, 768–783 (2019).
30. Otkin, J. A. et al. Assessing the evolution of soil moisture and vegetation conditions during the 2012 United States flash drought. *Agric. For. Meteorol.* **218–219**, 230–242 (2016).
31. Xi, X. & Yuan, X. Remote sensing of atmospheric and soil water stress on ecosystem carbon and water use during flash droughts over eastern China. *Sci. Total Environ.* **868**, 161715 (2023).
32. O, S. & Park, S. K. Global ecosystem responses to flash droughts are modulated by background climate and vegetation conditions. *Commun. Earth. Environ.* **5**, 88 (2024).
33. Christian, J. I. et al. Flash drought: A state of the science review. *WIREs. Water* **11**, e1714 (2024).
34. Mukherjee, S. & Mishra, A. K. A multivariate flash drought indicator for identifying global hotspots and associated climate controls. *Geophys. Res. Lett.* **49**, e2021GL096804 (2022).
35. Lovino, M. A., Pierrestegui, M. J., Müller, O. V., Müller, G. V. & Berbery, E. H. The prevalent life cycle of agricultural flash droughts. *npj Clim. Atmos. Sci.* **7**, 73 (2024).
36. Neelam, M. & Hain, C. Global flash droughts characteristics: Onset, duration, and extent at watershed scales. *Geophys. Res. Lett.* **51**, e2024GL109657 (2024).
37. Sehgal, V., Gaur, N. & Mohanty, B. P. Global Flash Drought Monitoring Using Surface Soil Moisture. *Water Resour. Res.* **57**, e2021WR029901 (2021).
38. Anderegg, W. R. L., Anderegg, L. D. L., Kerr, K. L. & Trugman, A. T. Widespread drought-induced tree mortality at dry range edges indicates that climate stress exceeds species' compensating mechanisms. *Glob. Change Biol.* **25**, 3793–3802 (2019).
39. Forzieri, G., Dakos, V., McDowell, N. G., Ramdane, A. & Cescatti, A. Emerging signals of declining forest resilience under climate change. *Nature* **608**, 534–539 (2022).
40. Sun, Y. et al. Drought onset mechanisms revealed by satellite solar-induced chlorophyll fluorescence: Insights from two contrasting extreme events. *J. Geophys. Res. Biogeosci.* **120**, 2427–2440 (2015).
41. Li, W. et al. Widespread increasing vegetation sensitivity to soil moisture. *Nat. Commun.* **13**, 3959 (2022).
42. Zhou, S., Yu, B., Huang, Y. & Wang, G. The effect of vapor pressure deficit on water use efficiency at the subdaily time scale. *Geophys. Res. Lett.* **41**, 5005–5013 (2014).
43. Liu, X., Feng, X. & Fu, B. Changes in global terrestrial ecosystem water use efficiency are closely related to soil moisture. *Sci. Total Environ.* **698**, 134165 (2020).
44. Ryu, Y. et al. Integration of MODIS land and atmosphere products with a coupled-process model to estimate gross primary productivity and evapotranspiration from 1 km to global scales. *Global Biogeochem. Cycles* **25**, GB4017 (2011).
45. Brookshire, E. N. J. & Weaver, T. Long-term decline in grassland productivity driven by increasing dryness. *Nat. Commun.* **6**, 7148 (2015).
46. Qing, Y., Wang, S., Yang, Z.-L. & Gentile, P. Soil moisture –atmosphere feedbacks have triggered the shifts from drought to pluvial conditions since 1980. *Commun. Earth. Environ.* **4**, 254 (2023).
47. Ustin, S. L. & Gamon, J. A. Remote sensing of plant functional types. *New Phytol.* **186**, 795–816 (2010).
48. Diaz, S. & Cabido, M. Plant functional types and ecosystem function in relation to global change. *J. Veg. Sci.* **8**, 463–474 (1997).
49. Wana, D. & Beierkuhnlein, C. Responses of plant functional types to environmental gradients in the south-west Ethiopian highlands. *J. Trop. Ecol.* **27**, 289–304 (2011).
50. Li, W. et al. Widespread and complex drought effects on vegetation physiology inferred from space. *Nat. Commun.* **14**, 4640 (2023).
51. Deng, Y. et al. Divergent seasonal responses of carbon fluxes to extreme droughts over China. *Agric. For. Meteorol.* **328**, 109253 (2023).
52. Gupta, A., Rico-Medina, A. & Caño-Delgado, A. I. The physiology of plant responses to drought. *Science* **368**, 266–269 (2020).
53. Kalra, A., Goel, S. & Elias, A. A. Understanding role of roots in plant response to drought: Way forward to climate-resilient crops. *The Plant Genome* **17**, e20395 (2024).
54. Zeng, X. Global Vegetation Root Distribution for Land Modeling. *J. Hydrometeorol.* **2**, 525–530 (2001).
55. Fan, Y., Miguez-Macho, G., Jobbágy, E. G., Jackson, R. B. & Otero-Casal, C. Hydrologic regulation of plant rooting depth. *Proc. Natl. Acad. Sci.* **114**, 10572–10577 (2017).
56. Petrik, P., Petek-Petrik, A., Mukarram, M., Schuldt, B. & Lamarque, L. J. Leaf physiological and morphological constraints of water-use efficiency in C3 plants. *AoB PLANTS* **15**, plad047 (2023).
57. Zhou, S. et al. Response of Water Use Efficiency to Global Environmental Change Based on Output From Terrestrial Biosphere Models. *Global Biogeochem. Cycles* **31**, 1639–1655 (2017).
58. Massenti, R. et al. Physiological and Structural Responses to Prolonged Water Deficit in Young Trees of Two Olive Cultivars. *Plants* **11**, 1695 (2022).
59. Farooq, M., Hussain, M., Ul-Allah, S. & Siddique, K. H. M. Physiological and agronomic approaches for improving water-use efficiency in crop plants. *Agr. Water Manage.* **219**, 95–108 (2019).
60. Christian, J. I. et al. A Methodology for Flash Drought Identification: Application of Flash Drought Frequency across the United States. *J. Hydrometeorol.* **20**, 833–846 (2019).
61. Yuan, X., Wang, L. & Wood, E. F. Anthropogenic intensification of southern African flash droughts as exemplified by the 2015/16 season. *Bull. Am. Meteor. Soc.* **99**, S86–S90 (2018).
62. Wang, L., Yuan, X., Xie, Z., Wu, P. & Li, Y. Increasing flash droughts over China during the recent global warming hiatus. *Sci. Rep.* **6**, 30571 (2016).
63. Mahto, S. S. & Mishra, V. Dominance of summer monsoon flash droughts in India. *Environ. Res. Lett.* **15**, 104061 (2020).
64. Fu, Z. et al. Sensitivity of gross primary productivity to climatic drivers during the summer drought of 2018 in Europe. *Phil. Trans. B* **375**, 20190747 (2020).
65. Joiner, J. & Yoshida, Y. Global MODIS and FLUXNET-derived Daily Gross Primary Production, V2. (ORNL DAAC, 2021).
66. Mohammadi, K., Jiang, Y. & Wang, G. Flash drought early warning based on the trajectory of solar-induced chlorophyll fluorescence. *Proc. Natl. Acad. Sci.* **119**, e2202767119 (2022).
67. Sehgal, V. & Mohanty, B. P. Preferential Hydrologic States and Tipping Characteristics of Global Surface Soil Moisture. *Water Resour. Res.* **60**, e2023WR034858 (2024).
68. Xia, Y., Ek, M., Wei, H. & Meng, J. Comparative analysis of relationships between NLDAS-2 forcings and model outputs. *Hydrol. Process.* **26**, 467–474 (2012).
69. Xia, Y. et al. Continental-scale water and energy flux analysis and validation for the North American Land Data Assimilation System project phase 2 (NLDAS-2): 1. Intercomparison and application of model products. *J. Geophys. Res. Atmosph.* **117**, <https://doi.org/10.1029/2011JD016048> (2012).
70. Barlage, M. et al. Noah land surface model modifications to improve snowpack prediction in the Colorado Rocky Mountains. *J. Geophys. Res. Atmosph.* **115**, <https://doi.org/10.1029/2009JD013470> (2010).

71. Wei, H., Xia, Y., Mitchell, K. E. & Ek, M. B. Improvement of the Noah land surface model for warm season processes: evaluation of water and energy flux simulation. *Hydrol. Process.* **27**, 297–303 (2013).
72. Rienecker, M. M. et al. MERRA: NASA's Modern-Era Retrospective Analysis for Research and Applications. *J. Clim.* **24**, 3624–3648 (2011).
73. Sheffield, J., Goteti, G., Wen, F. & Wood, E. F. A simulated soil moisture based drought analysis for the United States. *J. Geophys. Res. Atmosph.* **109** (2004).
74. Andreadis, K. M. & Lettenmaier, D. P. Trends in 20th century drought over the continental United States. *Geophys. Res. Lett.* **33**, <https://doi.org/10.1029/2006GL025711> (2006).
75. Martens, B. et al. GLEAM v3: satellite-based land evaporation and root-zone soil moisture. *Geosci. Model Dev.* **10**, 1903–1925 (2017).
76. Joiner, J. & Yoshida, Y. Satellite-based reflectances capture large fraction of variability in global gross primary production (GPP) at weekly time scales. *Agric. For. Meteorol.* **291**, 108092 (2020).
77. Rodell, M. et al. The Global Land Data Assimilation System. *Bull. Am. Meteor. Soc.* **85**, 381–394 (2004).
78. Mann, H. B. Nonparametric Tests Against Trend. *Econometrica* **13**, 245–259 (1945).
79. Kendall, M. G. Rank Correlation Methods. 4th Edition, Charles Griffin, London. (1975).
80. Sugihara, G. et al. Detecting Causality in Complex Ecosystems. *Science* **338**, 496–500 (2012).
81. Ye, H. et al. Equation-free mechanistic ecosystem forecasting using empirical dynamic modeling. *Proc. Natl. Acad. Sci.* **112**, E1569–E1576 (2015).

## Acknowledgements

S.W. acknowledges support from the Research Grants Council of the Hong Kong Special Administrative Region, China (Project No. PolyU/RGC 15232023) and the Hong Kong Polytechnic University (Project No. P0045957, P0043040).

## Author contributions

S.W. conceived and supervised the study. Y.J. carried out the analysis and drafted the manuscript. S.W. contributed to the interpretation and discussion of the results. P.W.C. and Z.L.Y. provided comments and suggestions for improving the quality of this paper.

## Competing interests

The authors declare no competing interest.

## Additional information

**Supplementary information** The online version contains supplementary material available at <https://doi.org/10.1038/s43247-025-02013-w>.

**Correspondence** and requests for materials should be addressed to Shuo Wang.

**Peer review information** *Communications Earth & Environment* thanks and the other, anonymous, reviewer(s) for their contribution to the peer review of this work. Primary Handling Editors: Heike Langenberg. A peer review file is available.

**Reprints and permissions information** is available at <http://www.nature.com/reprints>

**Publisher's note** Springer Nature remains neutral with regard to jurisdictional claims in published maps and institutional affiliations.

**Open Access** This article is licensed under a Creative Commons Attribution-NonCommercial-NoDerivatives 4.0 International License, which permits any non-commercial use, sharing, distribution and reproduction in any medium or format, as long as you give appropriate credit to the original author(s) and the source, provide a link to the Creative Commons licence, and indicate if you modified the licensed material. You do not have permission under this licence to share adapted material derived from this article or parts of it. The images or other third party material in this article are included in the article's Creative Commons licence, unless indicated otherwise in a credit line to the material. If material is not included in the article's Creative Commons licence and your intended use is not permitted by statutory regulation or exceeds the permitted use, you will need to obtain permission directly from the copyright holder. To view a copy of this licence, visit <http://creativecommons.org/licenses/by-nc-nd/4.0/>.

© The Author(s) 2025